Effect of hydrolysis on the phase evolution of water-based sol–gel hydroxyapatite and its application to bioactive coatings

D.-M. LIU*, T. TROCZYNSKI, D. HAKIMI
Department of Metals and Materials Engineering, University of British Columbia, Vancouver, BC, Canada V6T 1Z4

In a previous report, we demonstrated a successful synthesis of crystalline hydroxyapatite (HA) through the use of a water-based sol–gel process. It was shown that the apatite can be obtained at temperatures generally below 400 °C, providing a great advantage for practical bioactive coating purposes. The influence of hydrolysis of phosphorus sol solution on the phase evolution of the resulting HA is the focus of this investigation. Experimental results show that, in the absence of acid catalyst, a long-term hydrolysis, i.e. > 4 h, is required for better evolution of apatitic phase. Such a phase evolution is mainly attributed to an increased concentration of apatitic phase, rather than improved crystallinity in the calcined gels. With the aid of acid catalyst, we found that a well-crystalline HA can be synthesized over a time period shorter by 2–3 orders of magnitude than those without catalyst, i.e. a few minutes. In almost all cases, a small amount of tricalcium phosphate (TCP) was detected, which may be explainable by the formation of oligomeric derivatives of the phosphorus sol during synthesis, where calcium phosphate derivatives with lower Ca/P ratio than stoichiometry can be developed. By selecting an optimal sol as a dipping source, highly-porous dental root specimens were coated and a thin, dense, adhesive (upon finger-nail scratching test) coating was achieved after calcinations at 375 °C. An *in vitro* test also shows a bioactive character of the coating.

1. Introduction

Calcium hydroxyapatite (HA), either in bulk form or as a coating, has long been considered as one of the most attractive bioactive materials. The applications involve replacement, repair, and augmentation of disorder or defective hard or soft tissues, widely used in orthopedic and dental surgeries [1–4]. Chemical and structural resemblances between the natural apatite (i.e. mineralized bone) and synthetic HA allow strong chemical bonding to occur at the material–bone interface [5]. This results in a strong fixation of HA implants [6, 7] which is particularly critical over the early stage of post-implantation. The mineral phase in the natural bone consists mainly of ~ 70 wt % of poorly-crystalline apatite and a small amount of carbonated apatite. The poorly-crystalline HA, such as naturally-occurring apatite, is prone to be more soluble in physiological environment than that of highly-crystalline HA which is commonly considered to be non-resorable. There are several synthetic methods to form HA. However, due to brittleness of pure synthetic HA ceramics, either composite ([8] and the references therein) or coating [9] applications are frequently employed.

Among the synthetic schemes, the sol–gel route, which was introduced over a decade ago [10], has been receiving increasing attention, particularly for thin-film coatings [11–17]. In comparison to conventional methods, such as solid-state reactions [18] and wet precipitation [19], the sol–gel method provides a soft chemical route that ensures a significant improvement in the chemical and physical homogeneity of the resulting product. In the conventional sol–gel synthesis, metal alkoxides are frequently used as the starting materials. In this process the alkoxides are hydrolyzed in the presence of water, hydroxyl groups nucleophilically substitute alkyl groups bonded to the metal atom (M) and alcohol molecules (ROH) are released as byproduct:

$$\text{M–(OR)} + \text{H}_2\text{O} \rightarrow \text{M–(OH)} + \text{ROH} \qquad (1)$$

A subsequent polymerization–condensation reaction between M–(OH) molecules leads to the formation of –M–O–M– bond and water as a byproduct:

$$\text{M–(OH)} + \text{M–(OH)} \rightarrow \text{M–O–M} + \text{H}_2\text{O} \qquad (2)$$

Reactions (1) and (2) can be accelerated by acid or base catalysts. For most sol–gel glasses/oxides, reaction (2) proceeds spontaneously at room temperature to form

*Corresponding author.

a three-dimensional network structure, resulting in a solid-like gel. However, for orthophosphates, reaction (2) requires a moderate heat treatment to gel the sol solution [10, 12, 18]. Recently, a few examples demonstrated gellation of the orthophosphates at ambient environment if calcium ethoxide [10] or calcium glycolate [19] was employed as a starting material under highly acidic conditions.

A number of combinations between phosphorus and calcium of various chemical forms have been adapted for HA formation [11–21]. Triethyl phosphite has been widely used as one of the precursors because of its rapid hydrolysis, as opposed to trialkyl phosphate precursors. Subsequent interaction of the hydrolyzed phosphite with Ca precursors, for instance, calcium diethoxide [10], calcium acetate [20], or calcium acetate–glycolate [21], proceeds slowly to form Ca–P-containing derivatives. During the reactions, an increase in the coordination number of phosphorus from III to V was detected through ^{31}P NMR, an evidence of polymerization [10]. Non-aqueous solvents are frequently employed for dilution of triethyl phosphite, together with a small amount of water or acetic acid for hydrolysis. In the previous report [22], two of the present authors demonstrated a successful attempt to synthesize crystalline HA at relatively low temperatures of 300–400 °C, using water-based sol–gel process with the triethyl phosphite as one of the phosphorus precursors (the other was calcium nitrate). The low-temperature phase formation is capable of providing potential advantages for coating applications where certain oxidative degradation of underlying metal substrates (e.g. Ti or Ti alloys) ([23, 24] and the references therein) can be avoided or minimized when the coating is thermally treated in air.

According to previous experimental observations, triethyl phosphite is immiscible with water and forms emulsion phase after immediate mixing with water. The emulsion mixture turned into a clear solution after certain period of time, after which the phosphite odor disappeared, indicating a complete hydrolysis [25]. Westheimer *et al*. [25] proposed that the trialkyl phosphite proceeds rapidly to form dialkyl phosphate in acid, for instance, in the case of trimethyl phosphite, the unshared electron pair in trimethyl phosphite will react rapidly with proton to form protonated phosphite, followed by deprotonation to form a product:

$$\begin{aligned} &(CH_3OH)_3P : +H^+ \leftrightarrow (CH_3OH)_3P^+H \\ &(CH_3OH)_3P^+H + H_2O \rightarrow (CH_3O)_2P(H) \\ &\quad = O + CH_3OH + H^+ \end{aligned} \tag{3}$$

However, the chemistry of extended hydrolysis of dimethyl (or diethyl) hydrogen phosphite has not been fully identified. According to the reactions proposed by Masuda *et al*. [8], diethyl hydrogen phosphite underwent further hydrolysis or chemical modification to form monoethyl phosphite, followed by interaction with Ca to form a complex containing Ca and P. Crystalline HA then developed after heat treatment of the chemical complex at $> 600\,^{\circ}C$.

It is known that polymerization reaction will usually accompany hydrolysis. Therefore, a reaction to form oligomeric phosphorus compounds during synthesis is possible. This would result in the formation of calcium phosphate materials other than HA and accordingly, have a lower Ca/P ratio than stoichiometric HAp. Therefore, the main objective of this investigation is to study the effect of hydrolysis on the resulting phase evolution. The aim is to advance our understanding how (i) the time of hydrolysis affects phase evolution, (ii) the efficacy of phase formation will be modified by using acid catalyst. This knowledge is applied to process optimization, e.g. for deposition of HA coatings on Ti alloy substrates.

2. Experimental procedures

Fig. 1 shows schematically the flow chart of the synthesis procedure. Phosphorus sol was prepared by hydrolyzing small amount of triethyl phosphite (Fisher, USA) with distilled water in a paraffin-sealed glass container under vigorous stirring with and without the use of nitric acid, as catalyst. The molar ratio of phosphite/water is kept constant at 8. In the absence of the acid catalyst, the phosphite sol was hydrolyzed in water for 0.5, 1, 2, 4, 8, 16, and 24 h. In the presence of the catalyst, phosphorus sol solutions were prepared by adding 1 N, 2 N, and 5 N acid solution to phosphorus alkoxide. A second solution was prepared by dissolving stoichiometric amount (with resulting Ca/P molar ratio of 1.67) of calcium nitrate into distilled water to concentration of 2 M. The nitrate solution was added dropwise into the hydrolyzed phosphorus sol. The mixture was vigorously stirred for 10 min, followed by aging for 24 h at ambient environment. The pH value of the solution without acid was monitored during the hydrolysis and aging. The aged sol

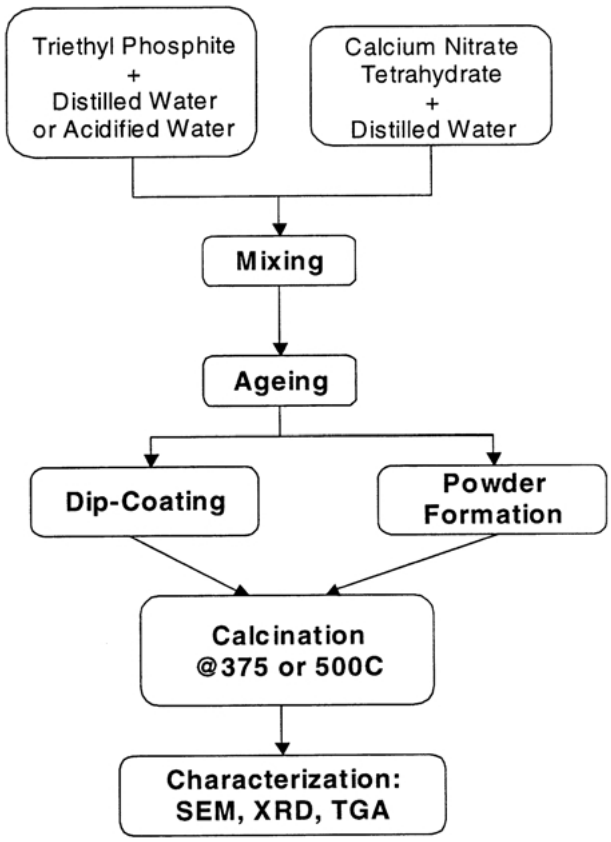

Figure 1 The flow chart of the synthetic scheme for the aqueous sol–gel hydroxyapatite synthesis.

was then oven dried at 80 °C until a dried gel was obtained. The white, dried gel was calcined at 375 °C for up to 6 h or at 500 °C for 10 min. Phase identification of the calcined powder was examined using X-ray diffraction (XRD, Rigaku Rotaflex 200, CuKα, Tokyo, Japan) with a scanning speed of 1° 2θ/min from $2\theta = 25°$ to 40°. The gel powders were also examined by thermal gravimetric analysis (Perkin Elmer, 7 series Thermal Analysis) to monitor the weight loss of organic residues. HA coatings were deposited by dipping commercial dental implants (Endopore Inc., Toronto, Canada) into the sol solution, followed by oven drying and calcination at 375 °C for 2 h in air. The microstructure of the gel powders and coatings was examined using scanning electron microscopy (SEM, Hitachi, S-800, Japan).

3. Results and discussion

3.1. Effects of hydrolysis time (systems without catalyst)

Fig. 2 shows the XRD patterns of the gels, hydrolyzed at different time durations, followed calcination at 375 °C for 4 h. The calcined gels showed a mixture of $CaCO_3$, calcium nitrate, and a small amount of apatitic reflections for a short term, i.e. 0.5 h and 1 h, hydrolysis. However, the gels showed a predominant apatitic structure together with a small amount of tricalcium phosphate (TCP) when the phosphite was hydrolyzed for ≥ 4 h. Several characteristic peaks, such as (0 0 2), (2 1 1), (1 1 2), (3 0 0), and (2 0 2) of the hydroxyapatite (JCPDS card #9-432) are clearly identified. The gelled powder after calcinations had dark gray color for those subject to short-term hydrolysis (SH) and was light gray for those subject to long-term hydrolysis (LH). An extended heating the light-gray LH gel for additional 2 h led to white color appearance again but still in gray color for the SH gels. This suggests that the LH gelled powders contained less amount of residues such as C_2H_5OH. A thermogravimetric analysis shown in Fig. 3 for both the SH and LH gelled powders provide quantitative evidence of the changes in the calcined powders. A relatively large weight-loss of about 16% was observed in the range of 25–100 °C for the LH powder, whilst the weight-loss was only about 5% for the SH powder. This weight-loss is primarily due to removal of adsorbed water and free solvent, i.e. most probably C_2H_5OH. Although both powders showed similar total weight-loss, i.e. $\sim 43\%$ above 550 °C, the weight-loss patterns the powders are different, indicating different pyrolytic mechanisms.

At the same temperature, for instance, 375 °C, the SH gelled powders demonstrated smaller weight loss ($\sim 12\%$), i.e. by about 13%, as compared to those of the LH powder ($\sim 25\%$). This means that the residues in the SH powder are more difficult to remove than in the LH ones. Therefore, it is reasonable to believe that sufficient amount of organic residues can still appear as chemically-bonded groups, such as C_2H_5O–, in the SH gelled powder and a higher temperature is required to remove them. This may also provide clue that a much stronger amorphous background was seen in the SH gel than that in the LH gel (Fig. 2). The increased XRD peak intensity with temperature is then suggestive of an increase in HA concentration and crystallite growth as well [22] rather than improved crystallinity, because the half-intensity width of the characteristic (0 0 2) peak remains unchanged for LH gels. However, an appreciable increase in the intensity and sharpness of the reflection peaks was revealed as depicted in Fig. 4 while

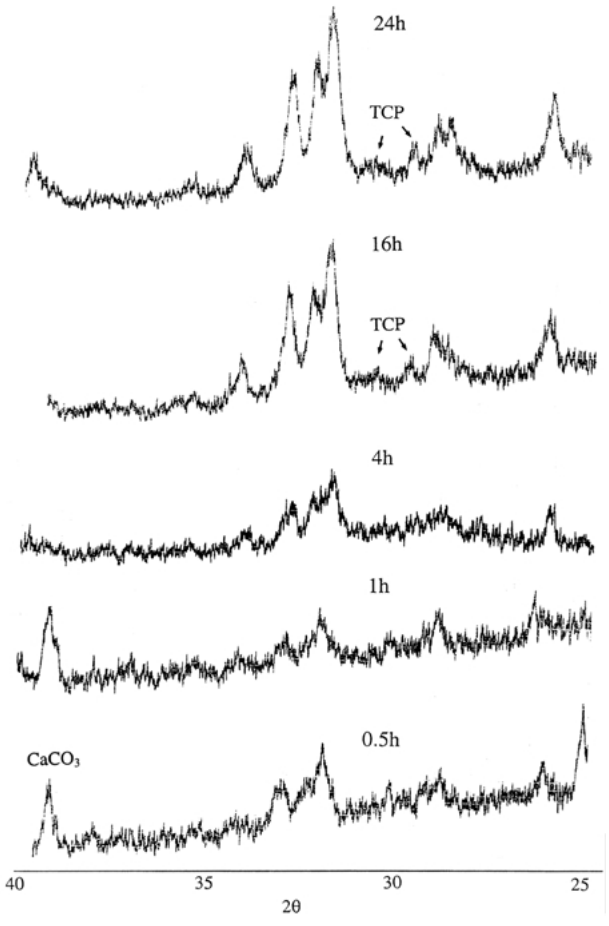

Figure 2 XRD patterns for the calcined gels (@ 375 °C) prepared under different time periods of hydrolysis of the phosphite sol, without acid catalyst.

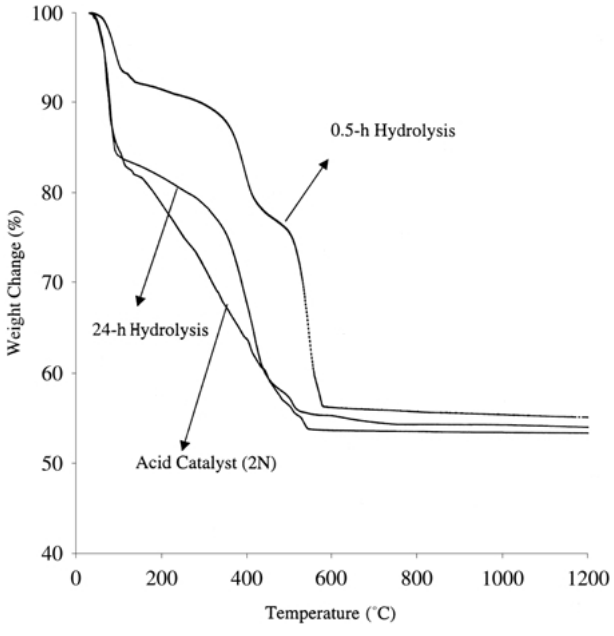

Figure 3 Thermal gravimetric analysis of the dried gels prepared under different conditions (with and without acid catalyst) of hydrolysis of the phosphite.

raising the calcinations temperature to 500 °C. This indicates an increase in HA concentration and improved crystallinity, as compared to those at 375 °C. Elemental analysis of the 500 °C-calcined gel using the energy dispersive spectroscopy (EDS) showed a Ca/P molar ratio of about 1.65–1.66, which is consistent with previous observation [22]. Therefore, it can be conceivable that the synthetic apatite could be a Ca-deficient apatite. The gels calcined at 500 °C showed white color in appearance, indicating no residues left. Small amount of TCP was detected for all the samples and the reflection intensity of the TCP peak was found to decrease with increasing time of hydrolysis. This indicates an extend hydrolysis favors HA formation. By monitoring the change in solution pH during the course of hydrolysis, Fig. 5 shows that the sol became more and more acid with time. The incorporation of more acidic phosphate ions, such as HPO_4^{2-}, rather than more basic group, PO_4^{3-}, into the resulting gel structure is more favorable (will be discussed later) and this may account for the decreased crystallinity (identified by the sharpness) of the apatitic peak.

The presence of TCP is unlikely to be a result of thermal decomposition of the apatitic phase initially developed because the calcinations temperature is too low (e.g. 375 °C) to destabilize the apatitic structure. One supporting evidence is that no appreciable change in the relative intensity of the major reflection peak between the

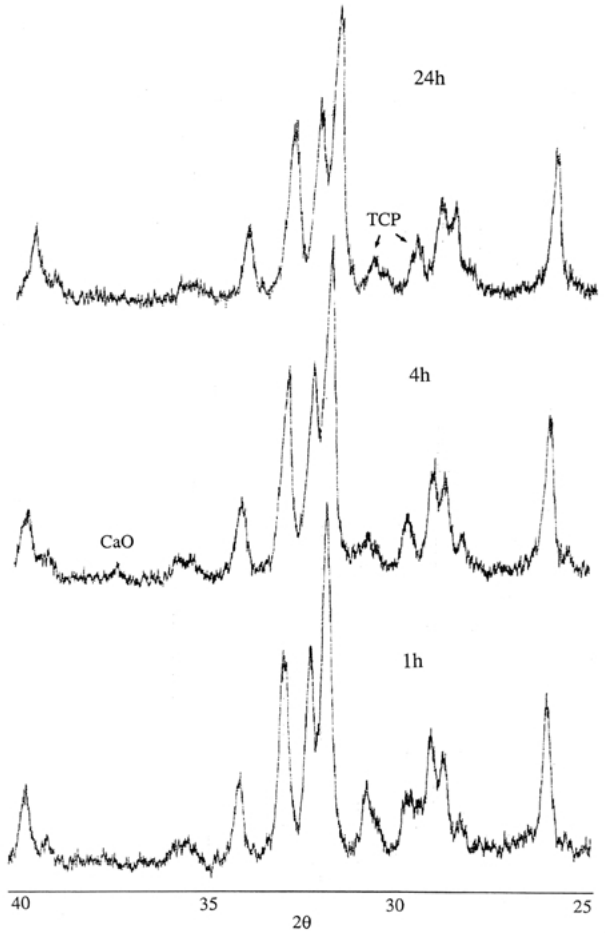

Figure 4 XRD patterns for the calcined gels derived from the phosphite sol under 1 h, 4 h, and 24 h hydrolysis. The gels showing similar apatitic phase evolution were calcined at 500 °C for only 10 min. A small amount of TCP was also detected in all cases.

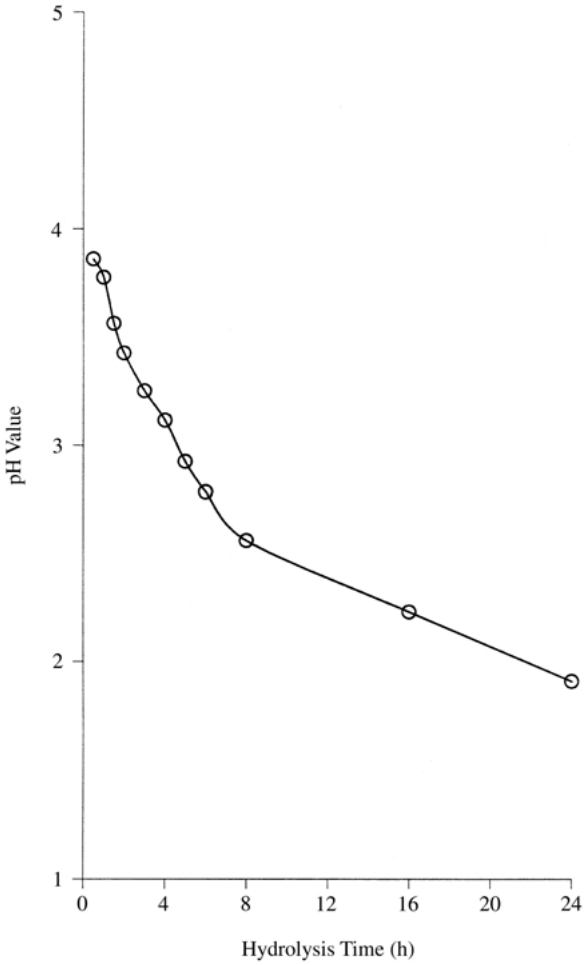

Figure 5 pH change in phosphite sol solution in terms of hydrolysis time.

TCP and apatite phase has been observed over an extended heating for 24 h at the same temperature, even after a higher temperature calcination at 500 °C (Fig. 4). The transformation from the Ca-deficient apatite to HA and TCP as indicated by Slosarczyk *et al.* [19] may be a possible alternative. However, the temperature used here is lower by 250–400 °C than that observed by Slosarczyk *et al.*, which accordingly is thermodynamically unfavorable to trigger the desirable reactions. However, if it does occur at such a low temperature region, then a detectable change in the relative intensity of the reflection peak between the TCP and HA phases should be easily observed. However, it can hardly be clearly distinguish from experimental observations. Therefore, one plausible explanation is a result of transformation from amorphous Ca–P-containing intermediate phases readily developed during synthesis. That is to say, a mixture of amorphous apatitic and TCP phase could be readily coexisting in the dried gel and transformed into crystalline phases upon thermal treatment. A mechanism to form oligomeric calcium phosphate derivatives is proposed in the later section, which seems accountable for the formation of low Ca/P calcium phosphates, such as TCP currently observed. As the main concern of this study, to obtain an HA gel with sufficient crystallinity and less amount of impurities, such as TCP and CaO, a sufficient time of hydrolysis seems necessary and from our observation, a time period of at least 4 h upon hydrolysis of the alkoxide phosphite is appropriate.

It is also interesting to note that the formation of apatitic phase becomes mush less time-dependent at 500 °C, however, stronger time dependence is observed at 375 °C. This is suggestive of a kinetically-controlled phase formation at lower temperatures, whilst thermodynamics dominating at higher temperatures. From the viewpoint of biocoating application, although a lower temperature treatment is always attractive for practical uses, it usually requires a prolonged thermal treatment, for instance, few hours [26], and is essentially deteriorate, by oxidative degradation, to the physical property of underlying metal substrate while performing in an oxygen-containing environment, e.g. ambient air. Furthermore, lower temperature provides little improvement in interfacial bonding between coating layer and metal substrate, which can lead to clinically fail after surgical operation. Therefore, it may be reasonable to believe that a relatively short-term dwelling, for instance, few minutes or even less, at somewhat higher temperature may be desirable for obtaining a well-crystalline and stronger adhesive apatitic layer.

3.2. Reactions during sol preparation

Triethyl phosphite can be hydrolyzed in the presence of water or air moisture to form diethyl phosphorus ester [10]:

$$P(OC_2H_5)_3 + H_2O \rightarrow HPO(OC_2H_5)_2 + C_2H_5OH \quad (4)$$

Masuda *et al*. [10] indicated that reaction (4) proceeds exceedingly slowly, for example, it takes 10 h or more to complete. However, a convenient and direct qualitative observation of the hydrolysis progress is the loss of phosphite odor, together with the disappearance of emulsion phase (present after initial mixing), to form a clear solution [25]. From our observation, all these can be achieved in about 20 min, which is in qualitative agreement with that reported by Westheimer *et al*. [25], suggesting that hydrolysis reaction should proceed vigorously to a greater extent over a time period that is much shorter than that observed by Masuda *et al*. [10]. A higher molar ratio of water to phosphite in our case (i.e. $r = 8$) may provide explanation for this discrepancy, where higher hydrolysis rate can be expected than that observed by Masuda *et al*. [10] (where $r = 1$ was studied). However, a continuous decrease in solution pH was detected for 24 h (Fig. 5), suggesting further progress of hydrolysis, by release of proton according to reaction (3). This strongly suggests that an extended hydrolysis of the diethyl phosphorus ester may undergo where more –OR groups were replaced by –OH groups:

$$HPO(OC_2H_5)_2 + H_2O \rightarrow HPO(OC_2H_5)_{2-x}(OH)_x + xC_2H_5OH \quad (5)$$

The hydrolyzed phosphite interacts with Ca ions in aqueous solution through a condensation polymerization reaction to form a Ca–P intermediate,

$$2\ HPO(OC_2H_5)_{2-x}(OH)_x + Ca^{++} \rightarrow \text{Ca–P intermediate} + 2H^+ \quad (6)$$

The liberation of proton in reaction (6) can be monitored by the change of the solution pH, as shown in Fig. 6, for the phosphite sol hydrolyzed for 4 h, where the solution pH decreases as a function of aging time for over a period of 24 h. This also indicates a slow reaction between hydrolyzed phosphite and Ca ions. Neither solid-like gel nor precipitate was ever observed for the sol solution aging for over 7 days. This may be accounted for by the partial charge model proposed by Livage *et al*. [27, 28], where the degree of the polymerization described in equation (6) must be low, resulting in oligomeric derivatives dispersed in solution, rather than a 3D network structure.

For the SH gelled powders, some organic ligands (e.g. alkyl groups) may still chemically bond to the phosphorus, e.g. $(OC_2H_5)_{2-x}O(H)P–O–Ca$, rather than being liberated as a byproduct, such as C_2H_5OH, which is much easier to burnout. The poor crystallinity of apatitic phase observed in Fig. 2 at lower temperatures also suggests that these residues may retard crystallization. The change in color and the phase evolution illustrated in Fig. 2 for the SH powders seems to be a supporting evidence. Instead, sufficient hydrolysis causes the formation of more free solvents (i.e. C_2H_5OH in reaction 5) and is expected to remove easily, resulting in a white-colored gel powder with improved crystallinity after extended calcination.

The presence of the TCP phase may be a result of condensation between hydrolyzed phosphite molecules to form oligomeric derivatives such as

$$2\ HPO(OC_2H_5)_{2-x}(OH)_x \rightarrow (OC_2H_5)_{2-x}O(H)P–\ O–\ P(H)O(OC_2H_5)_{2-x} + 2H_2O \quad (7)$$

The oligomeric derivative further hydrolyzes (reaction 8 below) and reacts with Ca to form calcium phosphate derivatives, reaction 9:

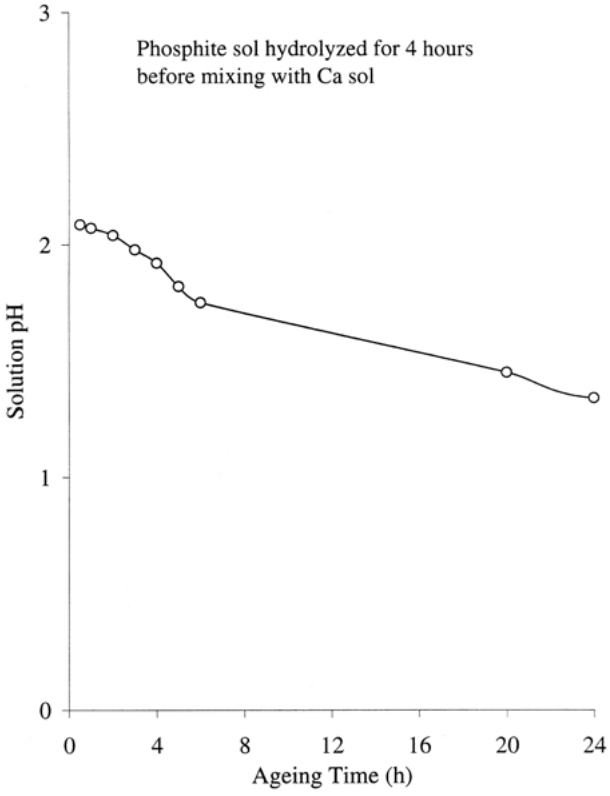

Figure 6 Solution pH in a mixed sol containing both Ca and P precursors after 24 h of aging.

$$(OC_2H_5)_{2-x}(H)OP\text{–}O\text{–}P(H)O(OC_25)_{2-x} + H_2O \rightarrow (OC_2H_5)_{2-y}(OH)_y\ (H)OP\text{–}O\text{–}P(H)O(OC_2H_5)_{2-y}(OH)_y + 2(x-y)C_2H_5OH \quad (8)$$

$$(OC_2H_5)_{2-y}(OH)_y(H)OP\text{–}O\text{–}P(H)O(OC_2H_5)_{2-y}(OH)_y + Ca^{--} \rightarrow Ca\text{–}O\text{–}(OC_2H_5)_{2-y}(H)OP\text{–}O\text{–}P(H)O(OC_2H_5)_{2-y}\text{–}O\text{–}Ca + 2H^+ + H_2O \quad (9)$$

Although above equations are of simplified and somewhat speculative chemical paths, they do propose the possibility for the formation of the Ca–P derivatives with lower Ca/P ratios than stoichiometry. In the XRD analysis, the lower Ca/P calcium phosphate presents in only a small amount in all cases, indicating that reaction (9), if it does occur, should not be extensively developed, but only relatively minor. Both the apatite and lower Ca/P calcium phosphate can be developed as amorphous complex intermediate in the gel, which then transformed into crystalline phases upon heating. The presence of tricalcium phosphate (Ca/P = 1.5) illustrated in Figs. 2 and 4 can be a supporting example. However, the exact chemical paths to form the TCP (or possibly other low Ca/P calcium phosphates that are undetectable under the resolution of the XRD) are not clearly understood at present.

Ironically, this ''impure'' TCP phase may be not an undesirable component on the basis of the biphasic calcium phosphate concept recently proposed by Daculsi [29]. From practical viewpoint, it is always desirable if an implant material can be designed in such a way that it can be completely replaced by the host tissues upon a resorption–apposition mechanism. Moreover, bioresorption has been a process that is able to accelerate the growth of defective hard tissues and this mechanism implies the significant role of resorption in biological response. Therefore, the non/less-resorbable nature of synthetic HA can be further modified by incorporation of more bioresorable second phase(s). Daculsi [29] took the advantage of the resorption/dissolution abilities of the different calcium phosphates (i.e. ACP or TCP) by combining more soluble tricalcium phosphate (TCP) with non- or less-soluble HA to form biphasic calcium phosphate (BCP). An optimization of dissolution balance was reported *in vitro* for the BCP. Therefore, an optimized combination of different calcium phosphates of varying degree of solubility may be a promising alternative for specific clinical purposes. Based on this concept, a minor fraction of the secondary TCP phase developed *in situ* under current synthesis conditions can be considered as an advantage rather than an obstacle.

3.3. Effect of acid catalyst

The use of acid catalyst to accelerate hydrolysis and/or polymerization is commonly exercised in conventional alkoxide-based sol–gel processes [28, 30]. The experimental observations in this work showed that an immiscible (emulsion-like) phosphite phase forms when the acid water was added. Subsequently the mix became a clear solution within a few seconds, accompanied with the loss of phosphite odor. However, it took about 20 min to obtain a clear, odor-free solution with distilled water alone (pH = 6.8). This means that the hydrolysis rate can be accelerated by 2–3 orders of magnitude when the acid catalyst is employed. Therefore, the time for hydrolysis described in previous section can reasonably be reduced by at least orders of magnitude, through use of acid catalysts. After performing a series of experiments, we have found that for these systems a time period of about 5 min is long enough for the development of crystalline HA. Fig. 7 shows the XRD patterns of the gelled samples prepared with acid catalyst of different concentrations, calcined at 375 °C for 4 h. The major apatitic peaks, e.g. (0 0 2), (2 1 1), (1 1 2), (3 0 0), and (2 0 2), are clearly distinguishable. The appearance of the calcined powders shows gray color for 1 N gel, indicating residues left and reduced relative concentration of the apatite phase. However, a white gel was seen for the 2 N and 5 N gels, indicating a minimum concentration of 2 N is necessary for such a short time period of hydrolysis. A comparative study of the XRD patterns between the powder (2 N) and the standard JCPDS file (not shown) showed that a small shift of the diffraction peaks (especially the characteristic peaks such as 0 0 2, 2 1 1, 1 1 2, 3 0 0, and 2 0 2) towards smaller 2θ by 0.06°–0.07°, relative to the standard

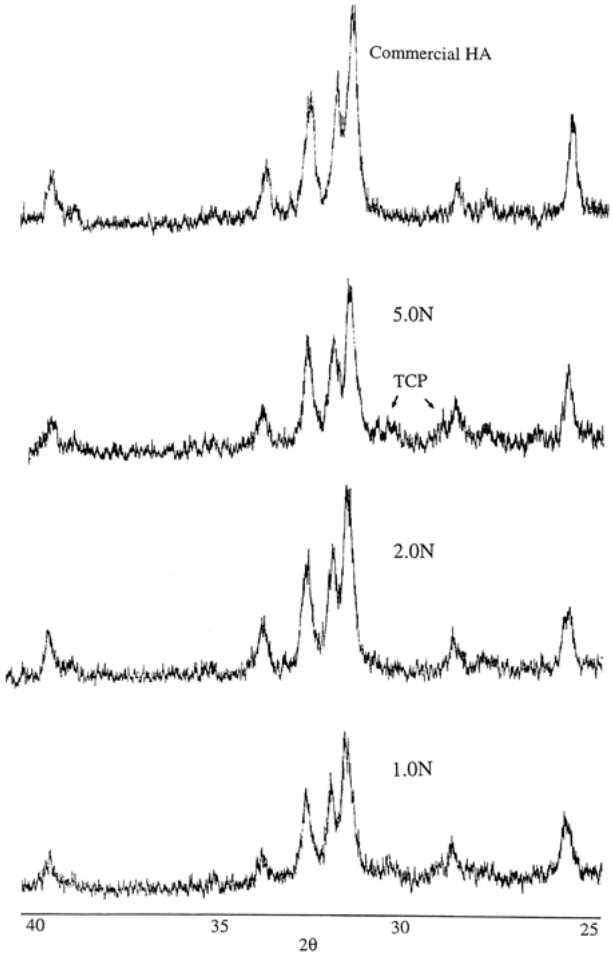

Figure 7 XRD patterns of the gels calcined at 375 °C. The gels were prepared under the presence of acid catalyst of different concentrations. A pattern corresponds to commercial HA is given for comparison purpose.

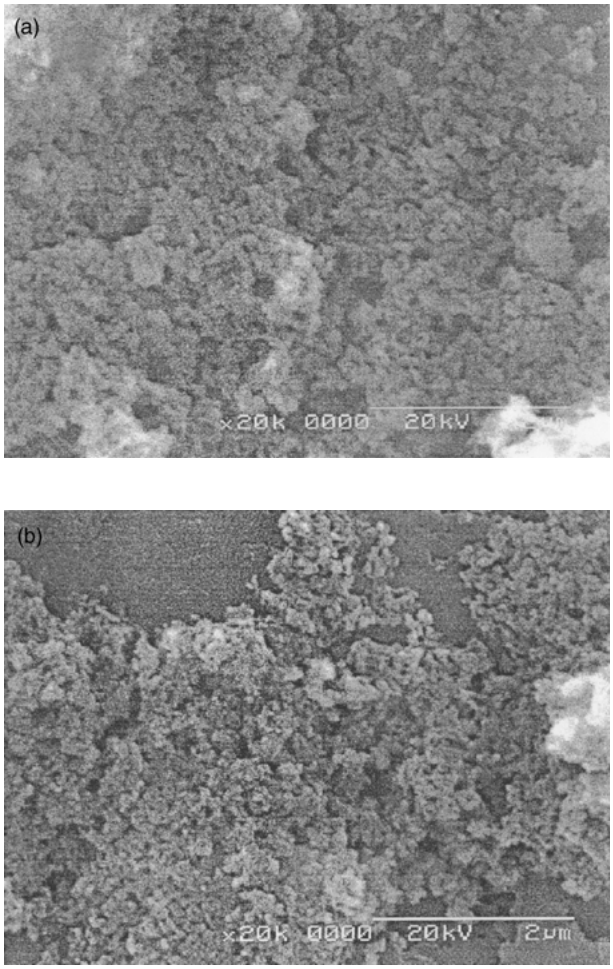

Figure 8 The morphology of the gel powders prepared (a) with and (b) without acid catalyst, after calcination at 375 °C.

pattern, was observed for the powder. This indicates an expansion in the crystal lattice along both *a* and *c* axes, indicating lattice imperfection by incorporation of larger ions. Accordingly, this defect may be introduced as a result of the higher acidity of the solution, where larger acidic phosphate HPO_4^{-2} may substitute smaller PO_4^{-3}, which may, based on electrical neutrality, have a chemical form of $Ca_{10-x}(HPO_4)_x(PO_4)_{6-x}(OH)_{2-x}$, i.e. a calcium-deficient apatite, which is agreed with the Ca/P ratio previously determined. Trace amount of TCP was also observed, but the one with 2 N catalyst shows little TCP phase and will be used for a subsequent coating practice.

It appears that hydrolysis (4) and polymerization reactions (5–8) can be concurrently taking place at a much faster rate with the aid of acid catalyst. The similar phase-evolution in these acid-catalyzed gels implies that the reaction paths can be similar to those without catalyst. The hydrolysis reactions (reactions 2 and 7) are believed to proceed more or less completely for the cases of higher acid content, i.e. ≥ 2 N. This results in more liberated C_2H_5OH and H_2O as y-products that can be removed easily during the subsequent heat treatment. However, a TGA curve of the acid-catalyzed (2 N) gelled powder shows a weight-loss behavior (in Fig. 3) somewhat different, in the temperature region of 100–430 °C, from those without catalyst, where a steady removal of the residues was observed, rather than a slow removal at 100–350 °C followed by a fast removal at 350–430 °C for the acid-free gels. The total weight-loss is higher by $\sim 1\%$ than those gels without catalyst, which is due to the presence of more nitrate from the acid. A greater extent of weight loss is always seen for the acid-catalyzed gel than the one without catalyst, suggesting the reactions proceeded more completely. However, the exact pyrolytic mechanism corresponding to the weight change pattern over the temperature region of 100–430 °C is not quite clear.

Microstructure examination revealed that both powders (with and without catalyst) calcined at 375 °C for 4 h show similar equi-axial geometry with particle size of about 120–150 nm, Fig. 8(a) and (b), respectively. The close resemblance of the particle morphology between both powders strongly suggests (i) the reaction paths during synthesis remaining unchanged and (ii) a particulate nature of the water-based sol–gel-derived apatite.

3.4. HA coatings on dental implants

Fig. 9(a) shows the porous-surface morphology of the dental implant (supplied by Endopore Inc., Toronto, Canada), composed of numerous Ti beads of 100–200 μm in diameter, attached to the solid core. Macropores ranging from few tens to about 150 μm can be observed between the beads. These macropores allow an ingrowth of bone tissue, providing interlocking for implant fixation and has been reported to receive good mechanical strength after implantation [31]. A thin layer of the sol–gel coating (~ 0.2 μm thick as estimated from a fractured surface, not shown) was deposited by single dipping the porous-surfaced dental implant into the acid-catalyzed solution (2 N), followed by oven drying. The coating was calcined at 375 °C in air for 2 h. Fig. 9(b) shows the surface morphology of the coating. The coating on the Ti beads is relatively smooth, in contrast to the previous investigation [22], where a porous, thicker coating was observed resulting from similar process. This is mainly attributed to the difference in solution concentration, i.e. a dilute one in the current study, as opposed to highly-concentrated solutions used in the previous study [22]. However, numerous cracks were observed in the coating in the necking area between Ti beads (arrows in Fig. 9(c)). This is due to the fact that the aqueous sol solution flowed down along the surface of the sphere during drying of the coating, and collected at the necking areas (and triple-junction areas as well) as a result of surface tension. In consequence, the layer on the sphere surface was relatively thin while those at the necking area substantially thicker, hence experiencing cracking and porosity. A closer look at the necking area shows that the pores have size ranging from approximately 1–5 μm, which may be advantageous for the circulation of physiological fluids. A thin and dense HA layer covers all other surface features of the Ti beads throughout the porous part of the implant. The dense, fine structure developed at such a low temperature suggests the ease of densification of the gel particles and is consistent with a number of sol–gel-derived oxides [30]. The test indicates that the aqueous sol–gel HA coating is suitable for biomedical devices having complex

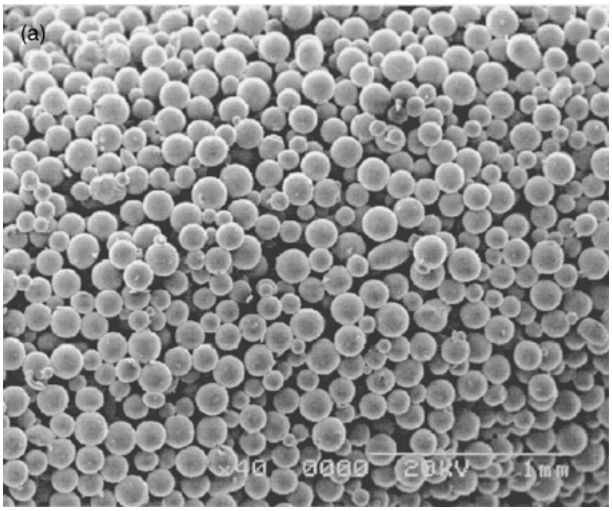

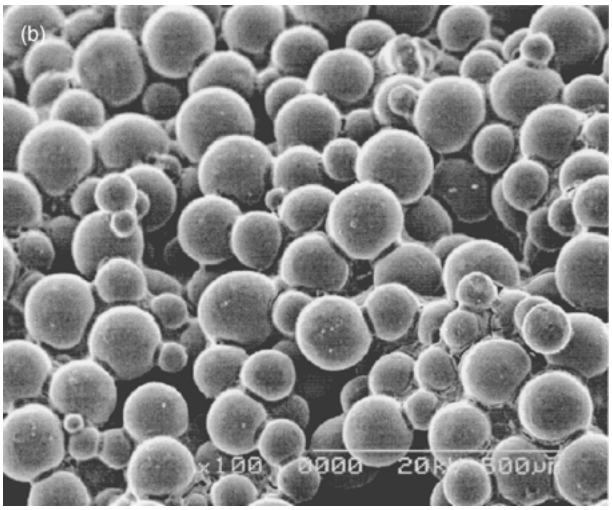

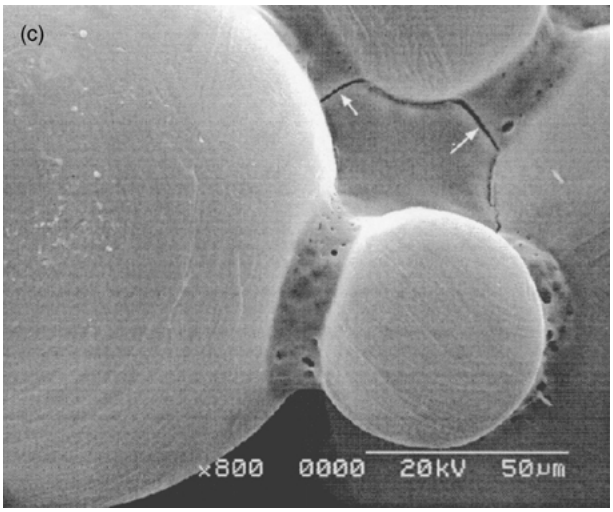

Figure 9 The morphology of the porous-surfaced dental root (a) before and (b) after sol–gel coating. A closer look of the coated surface (c) shows pores and cracks (arrows indicated) distributed along the neck and triple-junction areas. The surface feature of the underlying Ti beads can be observed and reproduced, indicating a thin, dense, and adhesive coating.

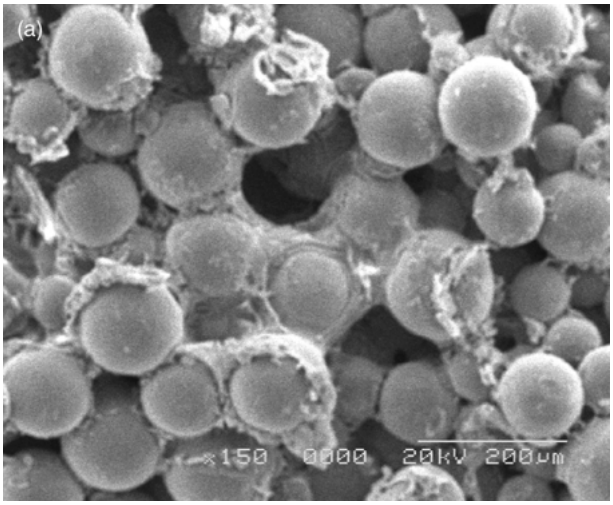

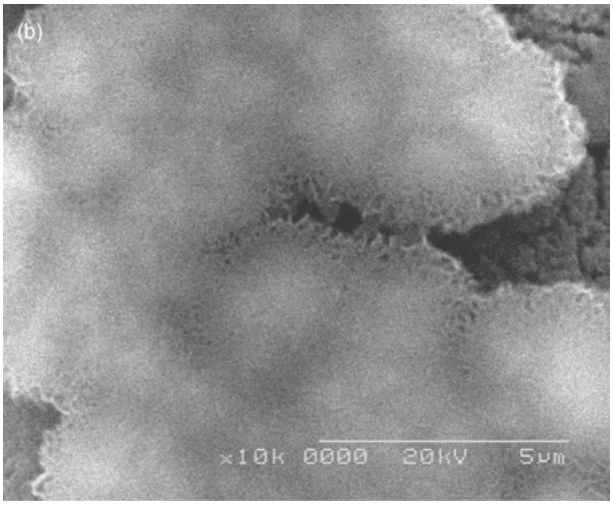

Figure 10 (a) Surface morphology of the sol–gel HA coated dental root after incubation in simulated body fluid at ambient for 7 days and (b) a closer look at the surface of the beads showing a deposited layer, exhibiting a microstructure similar to the formation of apatitic layer reported in literature.

geometry. In this respect, the HA coated surface reproduces the surface feature of the underlying porous titanium, retaining the bone interlocking capability of the surface. This is impossible to achieve using other coating techniques, e.g. through plasma spraying. It is interesting to note that the coating on the sphere surface is relatively thin and is electronically (also optically) transparent which allows the structural features of the underlying metal to be visually observed. A finger-nail scratching test was performed on the coated sample and showed nothing to come off from the sample surface. This, albeit somewhat qualitatively, does suggest an adherent coating.

By incubating the coated dental implant into a simulated body fluid, which has almost the same ionic components as those found in human blood plasma [32] for 7 days at ambient temperature. A layer of deposition was observed, as illustrated in Fig. 10(a) and a large magnification in Fig. 10(b). The deposited layer shows a microstructure similar to that observed in plasma-sprayed HA-coated samples [33] under similar *in vitro* test, an evidence of the formation of apatitic structure. This *in vitro* test suggests the bioactive nature of the aqueous sol–gel HA coating and a detailed *in vitro* investigation is currently underway and will be reported shortly.

4. Concluding remarks

The influence of hydrolysis of triethyl phosphite on the formation of hydroxyapatite via a water-based sol–gel route was investigated. A longer-term hydrolysis in distilled water ensures the formation of calcium phosphates with predominantly apatitic structure, formed at relatively low temperatures (i.e. 375 °C). Small amount of TCP evolved which is assumed to be a result due to oligomerization of the hydrolyzed phosphite upon synthesis. The hydrolysis and polymerization reactions proposed, although rather simplified, provided clues for some understanding on the formation of amorphous phases, and of the resulting crystalline HA and low Ca/P calcium phosphates, as substantiated to a certain extent by the XRD analysis. It has been shown that acid catalyst accelerates hydrolysis and polymerization reactions, which significantly shorten the time required for HA synthesis, as compared to the systems without the acid catalyst. By employing an optimal condition of the sol solution, a thin, dense coating can be achieved on porous-surface Ti dental devices at a temperature as low as 375 °C. The surface feature of the underlying Ti surface can be exactly reproduced suggesting an interfacial adhesion can be further improved by means of mechanical interlocking. This coating demonstrated bioactivity over a short time period of incubation in simulated body fluid at ambient temperature.

Acknowledgment

The authors thank the Natural Sciences and Engineering Council Canada for supporting of the work through UBC/VGH Engineering Orthopedics Research (T. Oxland, Director).

References

1. M. JARCHO, *Clin. Orthop.* **157** (1981) 259–278.
2. R. Z. LEGEROS, *Adv. Dent. Res.* **2** (1988) 164–168.
3. R. G. T. GEESINK, *Clin. Orthop.* **261** (1990) 39–58.
4. J. A. JANSEN, J. P. C. M. VAN DE WAERDEN, J. G. C. WOLKE and K. DE GROOT, *J. Biomed. Mater. Res.* **25** (1991) 973–989.
5. L. L. HENCH, *J. Am. Ceram. Soc.* **74** (1991) 1487–1510.
6. P. K. STEPHENSON, M. A. R. FREEMAN, P. A. REVALL, J. GERMAIN, M. TUKE and C. J. PIRIS, *J. Arthoplasty* **6** (1991) 51–58.
7. K. SOBALLE, S. OVERGAARD, E. S. HANSEN, H. BROKSTEAR-RASMUSSEN, M. LIND and C. BUNGER, *J. Long Term Eff. Med. Implants* **9**(1–2) (1999) 131–151.
8. W. SUCHANEK and M. YOSHIMURA, *J. Mater. Res.* **13**(1) (1998) 94–117.
9. P. DUCHEYNE and J. M. CUCKLER, *Clin. Orthopaedic Rel. Res.* **276** (1992) 102–114.
10. Y. MASUDA, K. MATUBARA and S. SAKKA, *J. Ceram. Soc.* Japan, **98** (1990) 1266–1277.
11. T. BRENDEL, A. ENGEL and C. RUSSEL, *J. Mater. Sci. Mater. Med.* **3** (1992) 175–179.
12. K. A. GROSS, C. S. CHAI, G. S. K. KANNANGARA, B. BIN-NISSAN and L. HANLEY, *ibid.* **9** (1998) 839–843.
13. S. W. RUSSEL, K. A. LUPTAK, C. T. A. SUCHICITAL, T. L. ALFORD and V. B. PIZZICOUI, *J. Am. Ceram. Soc.* **79**(4) (1996) 837–842.
14. L. D. PIVETEAU, M. I. GIRONA, L. SCHLAPBACH, P. BARBOUX, J. P. BOILOT and B. GASSER, *J. Mater. Sci. Mater. Med.* **10** (1999) 161–167.
15. D. B. HADDOW, P. F. JAMES and R. VAN NOORT, *J. Sol–Gel Sci. Tech.* **13** (1998) 261–265.
16. C. M. LOPATIN, V. PIZZICONI, T. L. ALFORD and T. LAURSEN, *Thin Solid Films* **326** (1998) 227–232.
17. C. S. CHAI and B. BEN-NISSAN, *Materials in Medicine* **10** (1999) 465–469.
18. R. A. YOUNG and D. W. HOLCOMB, *Calif. Tissue Int.* **34** (1982) 17–32.
19. A. SLOSARCZYK, E. STOBIERSKA, Z. PASZKIEWICZ and M. GAWLICK, *J. Am. Ceram. Soc.* **79** (1996) 2539–2544.
20. A. JILLAVENKATESA and R. A. CONDRATE, *J. Mater. Sci.* **33** (1998) 4111–4119.
21. W. WENG, L. HUANG and G. HAN, *App. Organometallic Chem.* **13** (1999) 555–564.
22. D. M. LIU, T. TROCZYNSKI and W. J. TSENG, *Biomaterials* **21** (2001) 1721–1730.
23. C. C. TING, S. Y. CHEN and D. M. LIU, *J. App. Physics* **88**(8) (2000) 4628–4633.
24. M. GUGLIELMI, *J. Sol–Gel Sci. Tech.* **8** (1997) 443–449.
25. F. H. WESTHEIMER, S. HUANG and F. CORITZ, *J. Am. Chem. Soc.* **110** (1988) 181–185.
26. M. SHIRKHANZADEH, *J. Mater. Sci. Mater. Med.* **60** (1995) 90–93.
27. J. LIVAGE, P. BARBOAX, M. T. VANDENBORRE, C. SICHMUTZ and F. TAULELLE, *J. Non-Cryst. Solids* **147/148** (1992) 18–23.
28. J. LIVAGE, M. HENRY and C. SANCHEZ, *Prog. Solid St. Chem.* **18** (1988) 259–341.
29. G. DACULSI, *Biomaterials* **19** (1998) 1473–1478.
30. C. J. BRINKER and G. W. SCHERER, ''Sol–Gel Science'', Chapter 2, (Academic Press Inc., London 1990).
31. C. A. SIMMONS, N. VALIQUETTE and R. M. PILLIAR, *J. Biomed. Mater. Res.* **47**(2) (1999) 127–138.
32. D. M. LIU, *Mater. Chem. Phys.* **36** (1994) 294–303.
33. D. M. LIU, H. M. CHOU and J. D. WU, *J. Mater. Sci. Mater. Med.* **5** (1994) 147–153.

Received 8 August 2000
and accepted 13 April 2001